Fine structure and magneto-optics of exciton, trion, and charged biexciton states in single InAs quantum dots emitting at 1.3 μm

N. I. Cade,* H. Gotoh, H. Kamada, and H. Nakano

NTT Basic Research Laboratories, NTT Corporation, Atsugi, 243-0198 Japan

H. Okamoto

NTT Photonics Laboratories, NTT Corporation, Atsugi, 243-0198 Japan

(Received 11 October 2005; revised manuscript received 17 November 2005; published 20 March 2006)

We present a detailed investigation into the optical characteristics of individual InAs quantum dots (QDs) grown by metalorganic chemical vapor deposition, with low temperature emission in the telecoms window around 1300 nm. Using microphotoluminescence (PL) spectroscopy we have identified neutral, positively charged, and negatively charged exciton and biexciton states. Temperature-dependent measurements reveal dot-charging effects due to differences in carrier diffusivity. We observe a pronounced linearly polarized splitting of the neutral exciton and biexciton lines (~ 250 μeV) resulting from asymmetry in the QD structure. This asymmetry also causes a mixing of the excited trion states which is manifested in the fine structure and polarization of the charged biexciton emission; from this data we obtain values for the ratio between the anisotropic and isotropic electron-hole exchange energies of $\widetilde{\Delta}_1/\widetilde{\Delta}_0 \approx 0.2$–$0.5$. Magneto-PL spectroscopy has been used to investigate the diamagnetic response and Zeeman splitting of the various exciton complexes. We find a significant variation in g factor between the exciton, the positive biexciton, and the negative biexciton; this is also attributed to anisotropy effects and the difference in lateral extent of the electron and hole wave functions.

I. INTRODUCTION

Semiconductor quantum dots (QDs) have attracted considerable attention in recent years as they exhibit novel optical and electronic phenomena,[1] which increasingly cannot be explained using an "artificial atom" type model.[2] High spatial resolution spectroscopy can provide a detailed insight into the nature of the confinement potential of individual dots and the quasiparticles that can form within them.[3] The creation of charged exciton states (trions) in QDs is of particular interest as these complexes are easily ionized in higher dimensional nanostructures. Over the last few years there have been many investigations into the properties of QD trions in both II-VI[4–6] and III-V[7–9] semiconductor materials; these studies have revealed a complex hierarchy of energies related to Coulomb, exchange, and correlation interactions between the constituent electrons and holes.[10,11]

The relative strengths of the isotropic and anisotropic parts of the electron-hole (*eh*) exchange are manifested in the fine structure splitting of the exciton state, which results from a reduction of the QD symmetry.[12,13] This effect can be studied in detail using magneto-optics;[14] however, to date there have been few investigations into the properties of magnetoexcitons in individual long-wavelength (>1 μm) QDs. Furthermore, the specific growth conditions required to produce these structures,[15] and their enhanced quantum-confinement,[16] are likely to have a significant effect on the carrier interaction energies. The development of semiconductor QD based devices for quantum optics and quantum information processing necessitates a detailed understanding of the nature of these interactions: the trion state has no fine structure and is therefore suitable for use as a single

photon source,[17] and the strength of the anisotropic *eh* exchange energy is an important issue in spin control systems.[18]

In previous studies the charge state of the QD has been varied using electrical injection of carriers[9,19,20] or photo-depletion effects.[21,22] However, with both techniques a comparative investigation of positive and negative charged species is complicated by requisite changes in the environmental conditions: in the former case the electrical field induces an emission Stark shift, and the latter case requires an increased carrier population. Here, we present the results of a comprehensive investigation into the optical characteristics of individual InAs QDs emitting at 1.3 μm; in addition to the formation of an exciton-biexciton system, we *simultaneously* observe recombination from positive and negative trion and biexciton states. These emission lines have relative intensities that are found to be highly sensitive to temperature due to diffusive dot-charging effects. Polarized photoluminescence (PL) spectroscopy shows that asymmetry induced fine structure and state mixing are present in the various exciton complexes, and from a systematic study of different dots we have quantified the magnitudes of the *eh* exchange energies. Finally we present a magneto-optical investigation of single QDs and we compare the diamagnetic shifts and Zeeman splittings of the neutral and charged complexes.

II. EXPERIMENT

The QDs investigated in this paper were fabricated by low-pressure metalorganic chemical vapor deposition (MOCVD) on a (100) GaAs substrate, using the dots-in-well (DWELL) technique:[23] a thin InAs dot layer (~ 1.7 monolay-
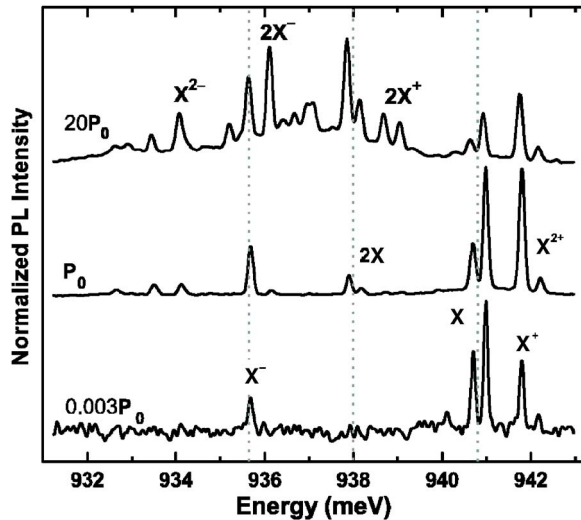
FIG. 1. (Color online) Normalized PL spectra from a single dot (QD1) in a 200 nm mesa at various excitation powers [E_{laser} =2.54 eV, P_0=5 W cm^{-2}]. Peaks X (2X) and $X^\pm$, $X^{2\pm}$ (2$X^\pm$) are attributed to neutral and charged exciton (biexciton) emission, respectively.

ers) was embedded in a 5 nm In$_{0.12}$Ga$_{0.88}$As(:Bi) quantum well (QW) and the whole DWELL heterostructure grown between GaAs barrier layers. The QD sheet density is estimated as 2×10^{10} cm^{-2} from atomic force microscopy (AFM) measurements on similar samples. More details of the growth procedure and general optical characteristics are presented in Ref. 24.

To perform single dot spectroscopy, mesa structures were fabricated by electron-beam lithography and dry etching. Zero-field micro-PL was taken from individual 200 $\times$200 nm^2 mesas excited by an Ar$^+$ laser (2.54 eV) focused to a $\sim$1 μm spot. Unless otherwise stated, the sample temperature was maintained at 5 K in a continuous-flow He cryostat. Magneto-PL measurements were performed at 10 K with the field aligned along the growth direction (Faraday geometry), using a diode laser (2.32 eV) focused to a $\sim$5 μm spot. The polarization of the luminescence was analyzed using a linear polarizer and quarter-wave retarding plate. In all cases the luminescence was dispersed in a 0.5 m spectrometer and detected using a nitrogen cooled InGaAs photodiode array (1024$\times$1).

III. RESULTS AND DISCUSSION

A. Power dependence, peak assignment, and thermal charging effects

PL spectra were taken from an individual mesa over a range of excitation powers spanning four orders of magnitude, as shown in Fig. 1. At low powers the spectra are composed of four narrow lines ($<$100 μeV, resolution limited); we have verified that all of these emission lines originate from a *single* dot in the mesa by comparing the PL spectra from many different mesas.[24] These lines show a linear increase in intensity over low excitation powers before saturating at $\sim$10 W cm^{-2} (2P_0), and they are attributed to

recombination from the exciton X and trion $X^\pm$ states. The exciton line shows a linearly polarized fine-structure splitting of approximately 300 μeV; this will be discussed further in the next section.

With increasing power additional lines appear below the exciton energy. In particular, the 2X doublet has a total intensity that is a quadratic function of excitation power, and this is assigned to the biexciton state. The binding energy of $\sim$3 meV is consistent with the values obtained by Kaiser *et al.*[25] for a similar strongly confined DWELL system. Other lines around 2X also show a superlinear intensity behavior; these are assigned to charged biexciton states 2$X^\pm$ formed by the capture of two *eh* pairs into a charged dot. The lowest energy features in Fig. 1 are attributed to multiply negatively charged states (X^{2-}, X^{3-}, etc.), each of which is split into a multiplet through electron-electron and electron-hole exchange interactions.[19,26]

Generally there are several possible origins for the excess carriers required for the creation of charged complexes: Nominally undoped GaAs structures usually have a residual background doping leading to impurities in the vicinity of a dot. However, these impurities will result in different emission spectra for each dot depending on the exact charge environment, whereas we obtain essentially identical spectra from many dots separated by millimeters on the sample. There is also no evidence of photodepletion effects that are typically observed in doped structures:[22] The positive and negative trion species seen in Fig. 1 are present for all excitation powers.

A second charging mechanism is the difference in carrier mobilities when *eh* pairs are generated in the GaAs barrier by nonresonant excitation. To investigate this effect PL spectra were taken with Ar$^+$ laser excitation (2.54 eV) from the same dot as Fig. 1 (QD1), over a range of temperatures; this is shown in Fig. 2(a). At 5 K the total integrated intensity of all the emission lines of one charge type is approximately equal for both positive and negative species (at power P_0); this suggests that the fluctuations in the excess charge within the dot are due to the random nature of the carrier capture process. With increasing temperature there is a successive transfer of emission intensity from the X^+ and X lines to the X^- and X^{2-} lines; this arises from an increase in the electron diffusivity relative to that of holes, effectively filling the dot with additional electrons.[8]

This thermally enhanced diffusion effect was confirmed by repeating the measurements using a yttrium aluminium garnet (YAG) laser (1.17 eV) to excite below the GaAs barrier and InGaAs QW energy [Fig. 2(b)]. In this case there is a monotonic decrease in intensity for all the trion lines with increasing temperature, due to the absence of diffusive dot filling from the GaAs. With YAG excitation, the presence of both charged exciton species in the PL seems inconsistent with a simple model of simultaneous *eh* photogeneration exclusively in the QD; however, the situation is complicated due to the nature of the DWELL structure: the interface between the QD and surrounding QW is not well defined and is the subject of current investigations. The YAG excitation energy is relatively close to the InGaAs QW emission energy ($\sim$1.24 eV, see Ref. 24), thence *eh* pairs may be created in QD states that are hybridized with low-energy states of the QW.[2]
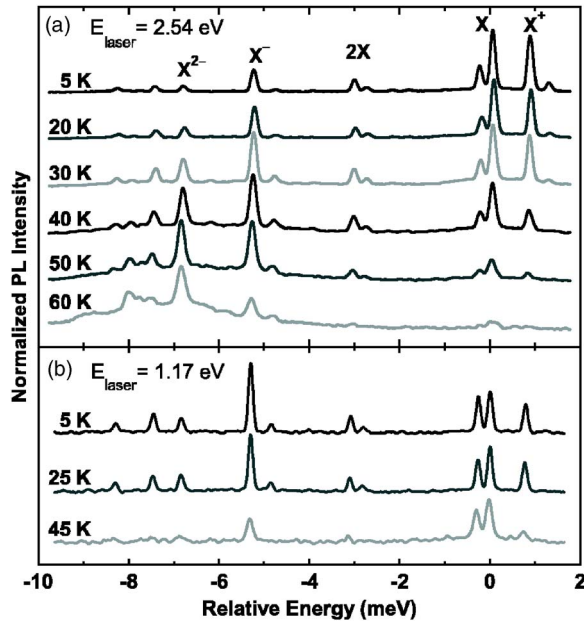
FIG. 2. (Color online) Normalized temperature-dependent PL spectra from QD1, with excitation (a) *above* the GaAs barrier and QW energy [2.54 eV, power P_0], (b) *below* the QW energy [1.17 eV, 200P_0]. In both cases the spectra have been shifted in energy to align the exciton X doublet, and offset vertically.

B. Polarization properties and fine structure

The heavy-hole exciton in zinc blende based quantum dots (D_{2d} point group) is fourfold degenerate and characterized by the angular momentum components $M = s_z + j_z = \pm 1, \pm 2$, where $s_z = \pm 1/2$ is the electron spin and $j_z = \pm 3/2$ is the hole angular momentum projection, respectively. The isotropic *eh* exchange interaction splits this quartet into a radiative doublet $|\pm 1\rangle$ (bright excitons) and two nonradiative singlets comprising combinations of $|\pm 2\rangle$ states (dark excitons), with a dark-bright exciton splitting Δ_0. An in-plane anisotropy, caused by, e.g., dot elongation and strain, will reduce the point group symmetry; this results in an additional splitting of the radiative doublet into the states $X_{a,b} = \frac{1}{\sqrt{2}}(|+1\rangle \mp |-1\rangle)$, separated by the anisotropic *eh* exchange energy Δ_1.[12]

Figure 3(a) shows polarized PL spectra from QD1, resolved along orthogonal axes using a rotatable polarizing prism. Both the X and the $2X$ emissions consist of a doublet with the two components linearly polarized along the Π_x and Π_y axes, which correspond closely to the (011) crystal axes. Both doublets have an identical splitting[27] and show a mirror symmetry in the polarization sequence. These observations are consistent with recombination from the spin-singlet $|0\rangle$ biexciton ground state to the bright exciton states X_a and X_b, with subsequent recombination to the $|0\rangle$ crystal ground state.[13,28] Furthermore, with the application of a magnetic field B there is a progressive evolution towards circularly polarized emission [Fig. 3(b)], as the mixed angular momentum states $X_{a,b}$ transform into pure $|\pm 1\rangle$ states.

In the trion ground state $X^\pm$ the two like-charges occupy the s shell with antiparallel spins and hence the exchange interaction energies are quenched. Consequently the Kramers
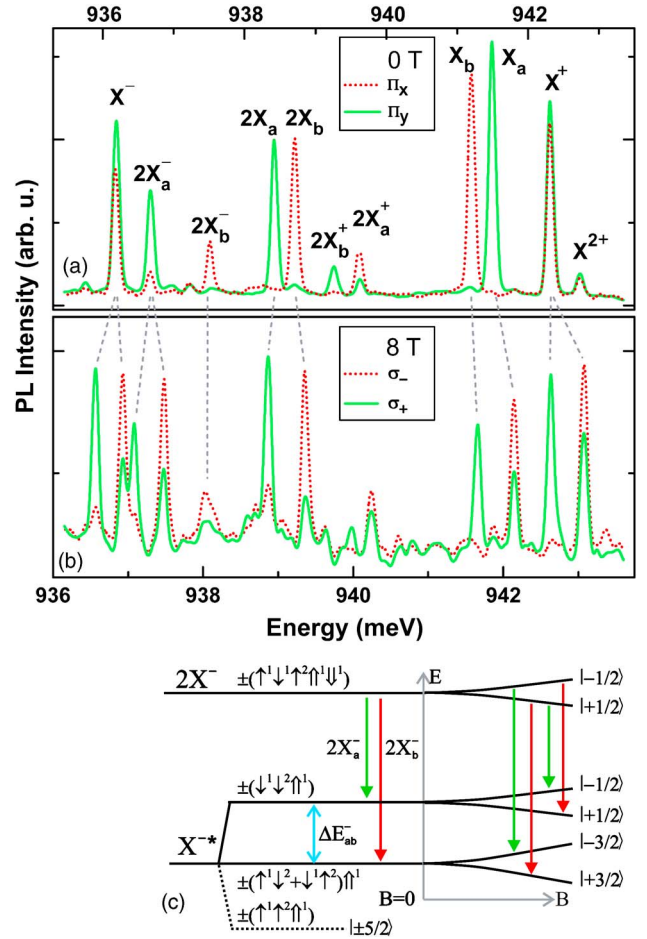

FIG. 3. (Color online) (a) Linearly polarized PL components from QD1 at zero magnetic field. (b) Circularly polarized PL components at $B = 8$ T. (c) Energy level diagram showing allowed transitions from the charged biexciton ground state to the trion triplet states, with and without a magnetic field applied in the growth direction. The spin projections of constituent electrons $s_z = \pm 1/2$ and holes $j_z = \pm 3/2$ are denoted by $\pm(\uparrow^l, \Uparrow^l)$, respectively, for the s shell ($l=1$) and p shell ($l=2$). The $2X^+$ has analogous transitions, except that the radiative X^{+*} states are transposed.

doublets are not split in the absence of a magnetic field even with a large dot asymmetry, and only one line is seen for each trion in Fig. 3(a).[29] However, in the excited or "hot" trion state $X^{\pm*}$ the additional charge resides in the p shell; the exchange energies are not quenched in this case and the spin-triplet state is split into a set of three Kramers doublets through the *eh* exchange interaction, as shown in Fig. 3(c). The emission lines $2X_a^-$ and $2X_b^-$ result from transitions between the $|\pm \frac{1}{2}\rangle$ charged biexciton ground state and the $|\mp \frac{1}{2}\rangle$ and $|\pm \frac{3}{2}\rangle$ X^{-*} triplet states, respectively. The total emission intensity ratio of $R_0 = I_b/I_a \approx 0.5$ is consistent with a smaller transition probability for $2X_b^-$, as the final $|\pm \frac{3}{2}\rangle$ state has a nonradiative component.[6] Furthermore, the incomplete linear polarization of these lines is direct evidence of state mixing caused by the anisotropic part of the *eh* exchange;[30] the larger degree of polarization for $2X_b^-$ as compared to $2X_a^-$ is again a result of the difference in transition probabilities. A similar analysis can be used to explain the characteristics of

the $2X_a^+$ and $2X_b^+$ emissions; R_0 is also ~ 0.5 for these lines, but their relative intensity and degree of linear polarization have a mirror symmetry to the $2X^-$ lines, as the radiative triplet states are transposed in X^{+*}.

The exchange energies in the $X^{\pm *}$ states will be different to those discussed above for the neutral exciton, due to the additional charge present in the p shell. Following the notation of Kavokin,[30] the total exchange energies in $X^{\pm *}$ are

$$\tilde{\Delta}_i = \frac{1}{2}(\Delta_i^1 + \Delta_i^2) \qquad (1)$$

for $i=0$ (isotropic component) and 1 (anisotropic component); the superscripts 1 and 2 represent the exchange energy of the first and second electrons (holes), respectively, with the hole (electron) in the X^{-*} (X^{+*}) state. For simplicity, we will continue to write $\Delta_1 \equiv \Delta_1^1$ unless explicitly required. The relative magnitudes of these exchange energies will be discussed below.

To gain a more detailed insight into the QD Coulomb energies, the emission spectra of 13 dots have been analyzed and are summarized in Fig. 4. For each dot the value of Δ_1 is shown in Fig. 4(a) plotted against the exciton energy.[27] The labels QD1–QD4 indicate the specific dots referred to throughout this report. There is no evidence of a direct correlation between Δ_1 and the X emission energy; however, as Δ_1 characterizes the asymmetry of the structure it is highly sensitive to dot shape, especially in small dots.[31]

For each dot, Fig. 4(b) shows the energies of the other exciton complexes relative to the center of the X doublet, plotted against the X emission energy. In all cases, the X^- (X^+) line appears at a lower (higher) energy than the exciton, which implies that the lateral extent of the single-particle wave function is smaller for the hole l_h than for the electron l_e.[21,32] A semiquantitative analysis of the binding energies of the exciton complexes has been performed: As the quantization energy is large for these dots (giving a total s-p shell splitting of ~ 90 meV),[24] it is possible to describe the charged excitons by treating the Coulomb interactions as perturbations to the single-particle states. Using the exchange integrals calculated by Warburton *et al.*[32] for a symmetric parabolic confinement potential, we find a reasonable agreement with the observed $X^\pm$ binding energies for $l_e \approx 7.5$ nm and $l_e/l_h \approx 1.3$. A full comparison with theory will require a more detailed knowledge of the size, shape, and composition of the dots.

There are obvious similarities in the binding energy trends in Fig. 4(b) for similar complexes. This is elucidated in Fig. 4(c) which shows the energy separation ΔE between different emission lines plotted against Δ_1 for each dot surveyed. Despite the relatively large range in the overall emission energy, ΔE for a pair of lines varies by <300 μeV among all the dots. This suggests that these QDs have a small size distribution, and the variations in X emission energy are primarily a result of fluctuations in the surrounding QW structure and process-induced strain effects.[33] For the negatively charged complexes there is a direct correlation between ΔE and Δ_1; in all cases the standard deviation from the solid best fit line is <100 μeV. In particular, the splitting between the
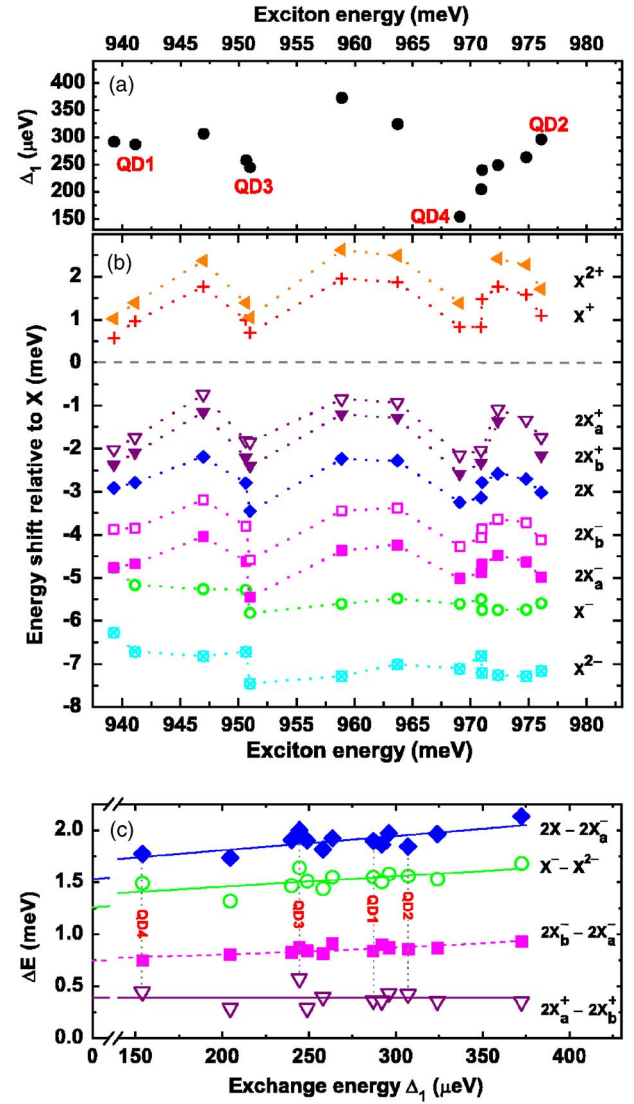

FIG. 4. (Color online) Summary of the PL characteristics of 13 single dots; QD1–QD4 indicate the dots referred to in the text: (a) Asymmetry induced fine-structure splitting Δ_1 plotted against exciton emission energy. (b) Emission energy of the exciton complexes relative to X, plotted against exciton emission energy. (c) Energy difference ΔE between emission lines in (b), as a function of Δ_1 for each dot. Solid lines are linear data fits; the bottom line has a gradient of zero. The dashed line is a fit using Eq. (2).

$2X_{a,b}^-$ doublet, shown in Fig. 3(c), is given by[6]

$$\Delta E_{ab}^- = \sqrt{(\tilde{\Delta}_0)^2 + 2(\tilde{\Delta}_1)^2}, \qquad (2)$$

which gives a close fit to the data in Fig. 4(c) (dashed line), where we have assumed that $\tilde{\Delta}_0$ is approximately constant for these dots and $\tilde{\Delta}_1 = \alpha \Delta_1$. We thence obtain values of $\tilde{\Delta}_0 = 0.75$ meV and $\alpha = 1.05$, and from Eq. (1) we find $\Delta_1^2/\Delta_1^1 \approx 1.1$. This slight enhancement in the $2e$-$1h$ anisotropic exchange energy compared with that of $1e$-$1h$ is probably a result of the $2e$ p-shell symmetry. For these dots the ratio between the anisotropic and isotropic eh exchange energies thence has values in the range $\tilde{\Delta}_1/\tilde{\Delta}_0 = 0.21$–$0.52$, which are

similar to the values obtained for charged dots in II-VI structures.[6]

In contrast to the $2X^-$, the positively charged biexciton $2X^+$ has a doublet splitting ΔE_{ab}^+ that appears to be insensitive to small variations in the dot asymmetry, as there is no obvious correlation with Δ_1. This is consistent with the smaller lateral extent of the hole wave function relative to that of the electron, as determined above. In general both $\widetilde{\Delta}_0$ and $\widetilde{\Delta}_1$ will differ between the $2X^-$ and $2X^+$, as the s-p exchange energies ($\Delta_{0,1}^2$) between $1e$-$2h$ and $2e$-$1h$ are sensitive to the exact shape and overlap of the carrier wave functions. A more detailed analysis would be facilitated by knowledge of the dark exciton energy levels using, e.g., Voigt configuration magneto-spectroscopy.[14]

C. Magnetophotoluminescence

The application of a magnetic field B can reveal additional information about a dot's confinement potential and electronic states, via the exciton diamagnetic response and spin splitting. In the absence of fine structure the field-dependent exciton emission energy is given by $E(B) = E_0 + \gamma_2 B^2 \pm \frac{1}{2} g_{ex}\mu_B B$, where E_0 is the zero-field emission energy, γ_2 is the diamagnetic coefficient, g_{ex} is the effective g factor of the exciton complex, and μ_B is the Bohr magneton. This field-dependent splitting is shown in Fig. 5(a) for the neutral and charged complexes in QD4. The preferentially left (σ^-) and right (σ^+) circularly polarized components are plotted as open and closed symbols, respectively, and the center position of each doublet is marked by a cross; a quadratic fit to these points is also shown by a solid line, from which γ_2 has been obtained.

With the inclusion of the anisotropic eh energy Δ_1 the Zeeman splitting for the X and $2X$ states is given by[34]

$$\Delta E_Z \equiv E(\sigma^+) - E(\sigma^-) = \sqrt{(g_{ex}\mu_B B)^2 + (\Delta_1)^2}, \quad (3)$$

where $E(\sigma^\pm)$ is the energy of the $\sigma^\pm$ polarized emission. This gives an excellent fit to the data in Fig. 5(b) from which we obtain values of g_X and g_{2X}. For the charged exciton complexes, g_{ex} can be found with a linear fit.

For excitons in strongly confined dots, where the quantization energy is larger than a typical Coulomb energy, γ_2 is dependent on the extent of the constituent carrier wave functions l_e and l_h; the diamagnetic shift is given by the difference in the shifts of the initial and final states, and will thus be identical for all exciton complexes with $1e$-$1h$ optical recombination. Figure 6(a) summarizes the values of γ_2 for the complexes seen in dots QD1–QD4. All four dots show a small diamagnetic shift ($<10\ \mu eV\ T^{-2}$) consistent with strong confinement; for each dot the neutral and charged states on the right of Fig. 6(a) have equal values of γ_2 to within $\sim 0.5\ \mu eV\ T^{-2}$, as expected. The larger variations in γ_2 for the charged biexciton complexes may originate from a small magnetic field dependence in the associated g factor, which will also introduce a quadratic B term that is indistinguishable from the diamagnetic response.

The values of g_{ex} shown in Fig. 6(b) are consistent with the results of Nakaoka *et al.*[35] for InAs dots fabricated with a
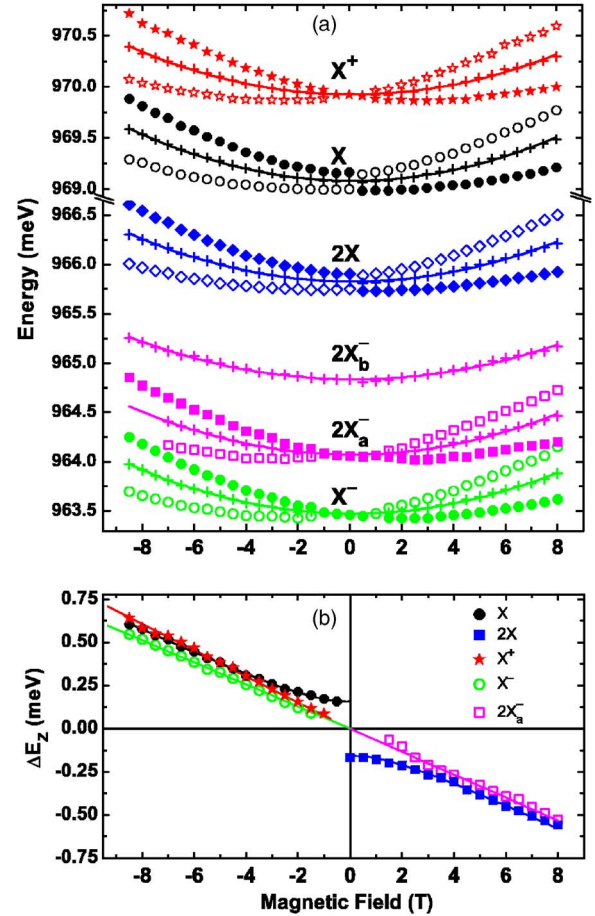

FIG. 5. (Color online) (a) Magnetic field dependence of the PL emission lines from QD4. Open (closed) symbols indicate preferentially σ^- (σ^+) polarized emission. Crosses mark the center of each doublet and the solid curves are quadratic fits. (b) Zeeman splitting ΔE_Z of the doublets in (a). The data for X and $2X$ have been fit using Eq. (3). For clarity, only the negative (positive) range has been plotted for X and $X^\pm$ ($2X$ and $2X^-$).

strain-reducing layer; the difference in g_X among the dots originates from size, shape, and strain variations. The degree of circular polarization seen in the spectra of each dot at 8 T is also consistent with the relative sizes of $g_X\mu_B B$ and Δ_1: QD1 and QD3 with smaller values of $|g_X|$ exhibit elliptically polarized emission even at 8 T, as seen in Fig. 3(a), whereas QD2 and QD4 emit almost completely circularly polarized light at $B = 4.5$ T.

In an isolated dot the trion g factor is predicted to be identical to that of the neutral exciton, as the excess carrier is present in the initial and final states of the transition;[36] this is seen for QD3 in Fig. 6(b). For the other dots studied the variations in g factor between X, $2X$, and $X^\pm$, although small, are still greater than the experimental error [as seen in Fig. 5(b)], and these variations show an identical trend in each case. The presence of dopants in the immediate vicinity of a dot might lead to perturbation of the band structure and a significant deviation in g factor between charged and neutral excitons;[37] however, the absence of any obvious emission from dark exciton states suggests that impurity-related valence band mixing effects are minimal for these dots,[28] as
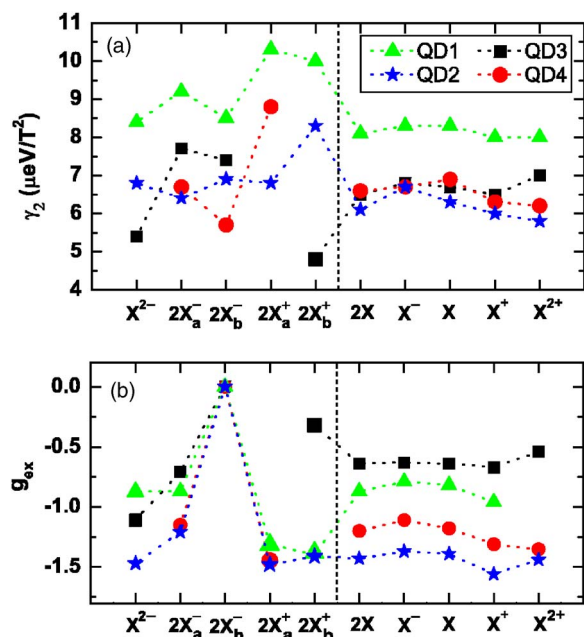
FIG. 6. (Color online) Summary of (a) the diamagnetic coefficient γ_2, and (b) the g factor g_{ex} of the exciton complexes, for QD1–QD4. Symbol size is greater than the absolute error in the data.

discussed in Sec. III A. It is likely that the variation between $g_{2X_a^-}$ and g_X is a result of state mixing caused by the anisotropic *eh* exchange; furthermore, the p shell electron may have a g factor that is sensitive to the specific confinement conditions.[6] Mixing of the bright $|\mp\frac{3}{2}\rangle$ and dark $|\pm\frac{5}{2}\rangle$ triplet states in the X^{-*} could be responsible for the anomalous zero splitting of the $2X_b^-$ line; this is unlikely to be a measurement error as it is observed for all four dots. However, a more detailed analysis has not been possible due to the weak emission intensity of the $2X_b^-$ line and the close proximity of other spectral lines. In contrast to the $2X^-$ lines, both $2X^+$ emission lines show relatively large spin splittings for three of the dots, which are approximately equal ($g_{2X^+} \approx -1.45$) and in-

dependent of g_X. This is consistent with the data in Fig. 5(c) which shows that the X^{+*} state mixing is relatively insensitive to variations in the dot shape, due to the smaller extent of the hole wave function.

IV. SUMMARY

We have analyzed the PL spectra of single InAs QDs grown by MOCVD using a strain-relieving DWELL structure. In addition to the formation of an exciton-biexciton system, we have simultaneously observed emission from both positive and negative trions and charged biexciton states at 5 K. The relative intensities of these lines are highly sensitive to temperature and we find a thermal dot-charging effect which is attributed to a difference in photogenerated carrier diffusivities. Analysis of the emission polarization reveals a large splitting of the X and $2X$ lines (250 μeV) due to the anisotropic electron-hole exchange interaction. The isotropic part of the exchange interaction also splits the excited trion triplet states, and gives rise to a mirror symmetry in the intensity and polarization degree of the charged biexciton emission doublets. From a study of the separation of the $2X^-$ lines in different dots, we have determined the ratio between the anisotropic and isotropic exchange energies. In contrast, the $2X^+$ doublet splitting appears uncorrelated with the degree of dot asymmetry; this is also manifested in the approximately constant g factor for these lines, determined by magnetospectroscopy. These effects are likely to be the result of differences in the shape and extent of the carrier wave functions, and warrant further investigation.

*Electronic address: ncade@will.brl.ntt.co.jp

[1] D. J. Mowbray and M. S. Skolnick, J. Phys. D **38**, 2059 (2005).

[2] K. Karrai, R. J. Warburton, C. Schulhauser, A. Högele, B. Urbaszek, E. J. McGhee, A. O. Govorov, J. M. Garcia, B. D. Gerardot, and P. M. Petroff, Nature (London) **427**, 135 (2004).

[3] A. Zrenner, J. Chem. Phys. **112**, 7790 (2000).

[4] B. Patton, W. Langbein, and U. Woggon, Phys. Rev. B **68**, 125316 (2003).

[5] V. Türck, S. Rodt, R. Heitz, O. Stier, M. Strassburg, U. W. Pohl, and D. Bimberg, Phys. Status Solidi B **224**, 217 (2001).

[6] I. A. Akimov, K. V. Kavokin, A. Hundt, and F. Henneberger, Phys. Rev. B **71**, 075326 (2005).

[7] M. Lomascolo, A. Vergine, T. K. Johal, R. Rinaldi, A. Passaseo, R. Cingolani, S. Patanè, M. Labardi, M. Allegrini, F. Troiani, and E. Molinari, Phys. Rev. B **66**, 041302(R) (2002).

[8] E. S. Moskalenko, K. F. Karlsson, P. O. Holtz, B. Monemar, W. V. Schoenfeld, J. M. Garcia, and P. M. Petroff, J. Appl. Phys. **92**, 6787 (2002).

[9] R. J. Warburton, C. Schaflein, F. Haft, F. Bickel, A. Lorke, K. Karrai, J. M. Garcia, W. Schoenfeld, and P. M. Petroff, Nature (London) **405**, 926 (2000).

[10] A. Zunger and G. Bester, Physica E (Amsterdam) **21**, 204 (2004).

[11] S. Rodt, A. Schliwa, K. Pötschke, F. Guffarth, and D. Bimberg, Phys. Rev. B **71**, 155325 (2005).

[12] M. Bayer, G. Ortner, O. Stern, A. Kuther, A. A. Gorbunov, A. Forchel, P. Hawrylak, S. Fafard, K. Hinzer, T. L. Reinecke, S. N. Walck, J. P. Reithmaier, F. Klopf, and F. Schafer, Phys. Rev. B **65**, 195315 (2002).

[13] V. D. Kulakovskii, G. Bacher, R. Weigand, T. Kümmell, A. Forchel, E. Borovitskaya, K. Leonardi, and D. Hommel, Phys.

Rev. Lett. **82**, 1780 (1999).

[14] M. Bayer, O. Stern, A. Kuther, and A. Forchel, Phys. Rev. B **61**, 7273 (2000).

[15] L. Seravalli, P. Frigeri, M. Minelli, P. Allegri, V. Avanzini, and S. Franchi, Appl. Phys. Lett. **87**, 063101 (2005).

[16] W.-S. Liu and J.-I. Chyi, J. Appl. Phys. **97**, 024312 (2005).

[17] S. M. Ulrich, M. Benyoucef, P. Michler, N. Baer, P. Gartner, F. Jahnke, M. Schwab, H. Kurtze, M. Bayer, S. Fafard, Z. Wasilewski, and A. Forchel, Phys. Rev. B **71**, 235328 (2005).

[18] M. Kroutvar, Y. Ducommun, D. Heiss, M. Bichler, D. Schuh, G. Abstreiter, and J. J. Finley, Nature (London) **432**, 81 (2004).

[19] J. J. Finley, P. W. Fry, A. D. Ashmore, A. Lemaitre, A. I. Tartakovskii, R. Oulton, D. J. Mowbray, M. S. Skolnick, M. Hopkinson, P. D. Buckle, and P. A. Maksym, Phys. Rev. B **63**, 161305#x0028;R) (2001).

[20] A. S. Bracker, E. A. Stinaff, D. Gammon, M. E. Ware, J. G. Tischler, D. Park, D. Gershoni, A. V. Filinov, M. Bonitz, F. M. Peeters, and C. Riva, Phys. Rev. B **72**, 035332 (2005).

[21] D. V. Regelman, E. Dekel, D. Gershoni, E. Ehrenfreund, A. J. Williamson, J. Shumway, A. Zunger, W. V. Schoenfeld, and P. M. Petroff, Phys. Rev. B **64**, 165301 (2001).

[22] A. Hartmann, Y. Ducommun, E. Kapon, U. Hohenester, and E. Molinari, Phys. Rev. Lett. **84**, 5648 (2000).

[23] L. F. Lester, A. Stintz, H. Li, T. C. Newell, E. A. Pease, B. A. Fuchs, and K. J. Malloy, IEEE Photonics Technol. Lett. **11**, 931 (1999).

[24] N. I. Cade, H. Gotoh, H. Kamada, T. Tawara, T. Sogawa, H. Nakano, and H. Okamoto, Appl. Phys. Lett. **87**, 172101 (2005).

[25] S. Kaiser, T. Mensing, L. Worschech, F. Klopf, J. P. Reithmaier, and A. Forchel, Appl. Phys. Lett. **81**, 4898 (2002).

[26] B. Urbaszek, R. J. Warburton, K. Karrai, B. D. Gerardot, P. M. Petroff, and J. M. Garcia, Phys. Rev. Lett. **90**, 247403 (2003).

[27] For each dot investigated, the difference between the X and $2X$ fine strucure splitting is <20 μeV, which is within the resolution error, and the mean value has been used.

[28] L. Besombes, K. Kheng, and D. Martrou, Phys. Rev. Lett. **85**, 425 (2000).

[29] J. J. Finley, D. J. Mowbray, M. S. Skolnick, A. D. Ashmore, C. Baker, A. F. G. Monte, and M. Hopkinson, Phys. Rev. B **66**, 153316 (2002).

[30] K. V. Kavokin, Phys. Status Solidi A **195**, 592 (2003).

[31] T. Takagahara, Phys. Rev. B **62**, 16840 (2000).

[32] R. J. Warburton, B. T. Miller, C. S. Dürr, C. Bödefeld, K. Karrai, J. P. Kotthaus, G. Medeiros-Ribeiro, P. M. Petroff, and S. Huant, Phys. Rev. B **58**, 16221 (1998).

[33] H. Qiang, F. H. Pollak, Y.-S. Tang, P. D. Wang, and C. M. Sotomayor Torres, Appl. Phys. Lett. **64**, 2830 (1994).

[34] M. Bayer, A. Kuther, A. Forchel, A. Gorbunov, V. B. Timofeev, F. Schafer, J. P. Reithmaier, T. L. Reinecke, and S. N. Walck, Phys. Rev. Lett. **82**, 1748 (1999).

[35] T. Nakaoka, T. Saito, J. Tatebayashi, S. Hirose, T. Usuki, N. Yokoyama, and Y. Arakawa, Phys. Rev. B **71**, 205301 (2005).

[36] C. Schulhauser, A. Högele, A. O. Govorov, R. J. Warburton, K. Karrai, J. M. Garcia, D. B. Gerardot, and P. M. Petroff, Physica E (Amsterdam) **25**, 233 (2004).

[37] M. Bayer, A. Kuther, F. Schafer, J. P. Reithmaier, and A. Forchel, Phys. Rev. B **60**, R8481 (1999).